IEEE Access
Multidisciplinary | Rapid Review | Open Access Journal

Received 11 August 2026, accepted 20 August 2026, date of publication 25 August 2026, date of current version 4 September 2026.

Digital Object Identifier 10.1109/ACCESS.2026.3727498

APPLIED RESEARCH

A Condition-Aware Data-Driven Framework for Tire–Road Noise Estimation Under Limited Data Conditions

M. DEMETGÜL, M. HEINZELMANN, AND S. LAZAROVA-MOLNAR
Institute of Applied Informatics and Formal Description Methods (AIFB), Karlsruhe Institute of Technology (KIT)—Karlsruhe Institute of Technology, 76133 Karlsruhe, Germany

Corresponding author: M. Demetgül (mustafa.demetguel2@kit.edu)

This work was supported in part by KIT Open Access Publication Fund, and in part by the ''Tire Road Noise'' Project funded by the Federal Ministry for Transport (BMV) as part of the mFUND Innovation Initiative.

ABSTRACT Tire–road noise is a major contributor to traffic noise and is strongly influenced by tire properties, road surface characteristics, and driving conditions. Accurate estimation of tire–road noise remains challenging, especially under limited data availability and varying operating conditions. This study proposes a condition-aware data-driven framework for tire–road noise estimation based on multi-sensor measurements. The proposed approach integrates On-Board Sound Intensity (OBSI), tire cavity noise, and vehicle CAN bus signals using a multi-scale feature extraction strategy. One-third-octave Sound Pressure Level (SPL) representations are employed to capture the dominant spectral characteristics of tire–road interactions. To improve model stability and reduce overfitting under limited-data conditions, an ensemble learning framework is adopted. In addition, a Leave-One-Group-Out (LOGO) validation strategy is used to ensure realistic performance evaluation across different tires, road surfaces, speeds, and acceleration scenarios. Multi-task learning is applied to jointly estimate OBSI and tire cavity noise. Experiments are conducted using four instrumented vehicles and multiple tire types under standardized road conditions. The results indicate stable and consistent performance across diverse operating conditions, particularly within the 400–5000 Hz frequency range where tire–road noise energy is most dominant. Overall, this work provides a condition-aware and reproducible data-driven methodology for tire–road noise estimation and provides a basis for future large-scale monitoring and data-driven noise analysis applications.

INDEX TERMS Ensemble learning, LOGO, multi-sensor fusion, OBSI, tire–road noise, tire cavity noise.

I. INTRODUCTION

Noise is an environmental stressor, generally defined as unwanted sound [1]. Furthermore, environmental noise is an independent risk factor for cardiovascular disease and is recognized as a public health threat by the World Health Organization [2], [3]. Tire-road noise has become the dominant source of traffic noise [4], [5]. Therefore, reducing tire-road noise is an important step to improve driving comfort and reduce urban noise levels [6].

To address this problem, it is essential to understand the physical mechanisms responsible for tire–road noise generation. Tire–road noise is generated by two main mechanisms: mechanical and aerodynamic [7]. Mechanical noise results from vibrations of the tire structure caused by road surface irregularities, where pavement texture and tread pattern excite the tire and make it radiate sound. Aerodynamic noise is mainly caused by air pumping in the tread grooves, together with effects such as pipe resonance, Helmholtz resonance, and horn amplification, which further increase the radiated noise [8], [9], [10]. The interaction of these mechanisms leads to complex, frequency-dependent noise characteristics, making accurate modeling challenging.

The study of tire–road noise relies on specialized measurement techniques designed to capture these mechanisms. Measurement approaches can be broadly classified into wayside noise measurements and noise measurements at the source. Wayside methods include coast-by, statistical pass-by,

The associate editor coordinating the review of this manuscript and approving it for publication was Xuebo Zhang.

controlled pass-by, acceleration pass-by, and continuous-flow traffic measurements, where microphones are placed at fixed distances and heights to record vehicle noise as it passes [11], [12]. In contrast, source-based methods such as CPX, OBSI, and the laboratory drum method measure tire–pavement noise close to the tire, reducing external interference [13], [14], [15]. CPX uses microphones positioned near the tire to measure sound pressure, while OBSI measures sound intensity with microphones placed even closer to the tire, resulting in higher measured levels [16]. The laboratory drum method performs measurements in a controlled environment using a rotating drum that replicates road surface texture. These measurement methods form the basis for subsequent signal processing and modeling.

Signal processing plays a central role in the measurement, analysis, and prediction of tire–road noise. Raw acoustic signals obtained from CPX, OBSI, or coast-by measurements contain components generated by mechanical and aerodynamic mechanisms and therefore require transformation and filtering to extract meaningful information. Sound Pressure Level (SPL) is a logarithmic measure of sound pressure and is commonly used in tire–road noise studies [17], while Sound Intensity Level (SIL) is used in the OBSI approach [17]. Frequency-domain analysis is typically performed using the Fast Fourier Transform (FFT) [18], and time–frequency methods such as STFT, Wavelet Transform, Wigner–Ville Distribution, Hilbert Transform, and Empirical Mode Decomposition are applied to analyze non-stationary signals [19]. One-third-octave band analysis is also widely used to represent sound spectra in standardized frequency bands for tire–road noise prediction, with different frequency ranges reported in the literature [20], [21]. Filtering, adaptive signal processing, and data fusion techniques are further applied to improve signal quality and support vibroacoustic analysis [19].

To effectively reduce tire-road noise, it is crucial to understand and accurately predict the mechanisms of its generation [22]. For this purpose, various modeling approaches have been proposed in the literature. Deterministic models describe noise generation and provide high interpretability but require considerable calculation effort and detailed input parameters [23]. In contrast, statistical models infer empirical relationships between measured noise levels and influencing factors and offer computational efficiency at the expense of physical transparency [24]. Previous studies have identified vehicle speed, tire characteristics, and pavement texture as key influencing factors for tire–road noise. Hybrid models combine these two approaches but often require large datasets for effective training [25].

Early studies on tire–road noise mainly used experimental measurements and simple statistical models. These studies showed that road surface texture, tire type, and vehicle speed strongly affect the sound pressure level (SPL) [26], [27], [28]. Later, machine learning and deep learning methods were introduced, and ANN and CNN models reduced the prediction error to about ±1.5–1.85 dB [18], [29], [30]. However, although these models improved accuracy, they did not clearly explain the physical reasons behind the noise. More recent studies have focused on hybrid and physics-informed deep learning models, often using data from multiple sensors, and reported much higher accuracy with R^2 values above 0.93 [11], [25], [31], [32], [33]. In contrast, this study focuses on data-driven tire–road noise estimation under limited-data conditions using measured signals and physically meaningful acoustic representations, with particular emphasis on generalization to unseen operating conditions. However, despite these improvements in prediction accuracy, most studies evaluate their models under limited experimental settings, and their ability to generalize to unseen tires, road surfaces, vehicle speeds, and operating conditions remain insufficiently investigated. This limitation is particularly important for real-world tire–road noise prediction, where models are expected to maintain robust performance across diverse operating conditions.

Most studies applied purely statistical approaches by feeding tread pattern images directly into CNNs instead of using physical processing [11], [30]. Lee et al. reported that this approach removed the need for 3D tire scans and improved prediction accuracy from 75% to 89% [30], while Mohammadi et al. found it inferior to their hybrid RVM-based model [11]. Che et al. used simple tread pattern parameters with a genetic algorithm to predict third-octave bands with an average error of 1.4% [13], [34]. Other studies focused on individual factors such as speed, pavement texture, or tire cavity noise rather than tread patterns [14], [26], [35]. Overall, many existing studies remain limited in scope, often considering only a small number of parameters, a single tire or road surface, or partial noise components.

Representative examples of hybrid approaches include the work of Mohammadi et al. modeled the main tire–road noise mechanisms individually [8] and later replaced the most expensive texture impact model with a statistical one, resulting in a fast hybrid approach using SVM and Relevance Vector Machine (RVM) [25]. Hybrid and statistical models have also been developed using linear and multiple regression [13], [35], grey models [36], pattern recognition [37].

A key difference between purely statistical and hybrid models is how the tire tread pattern is processed. In hybrid approaches, tread pattern noise is modeled using power spectra that represent mechanical mechanisms (tread pattern) and aerodynamic effects (air velocity), which are then used as inputs to ANN models [11], [29], [30], [38]. Li et al. showed a strong correlation between these spectra and tread pattern noise, but also noted that this contribution is generally small for most tires, except snow tires [29].

Several studies applied this concept using laboratory drum measurements in the context of tire design. Lee et al. extracted parameters from tread pattern power spectra derived from 3D tire scans and achieved 75% prediction accuracy for pattern noise using an ANN [30]. Rapino et al. used a single tread pattern power spectrum together with operating and tire parameters to predict one-third-octave bands from 200 Hz to 4000 Hz with an RMSE of 2.3 dBA [21]. Spies et al. employed a hybrid model with two ANNs to separately predict tread pattern and non–tread pattern noise, incorporating speed effects through scaling laws, and achieved an average total noise error of 1.1 dB [38].

Recent studies have explored both hybrid and purely data-driven approaches for tire–road noise prediction [39]. These studies demonstrate the increasing use of artificial intelligence for tire–road noise prediction, both within hybrid architectures [21], [38] and as purely data-driven models based on sensor measurements or tire image inputs [11], [29]. However, most studies have focused on single tires, constant speeds, limited vehicle and road conditions, or controlled laboratory environments.

Several recent studies within the Tire Road Noise research project have addressed complementary aspects of tire–road noise monitoring. Cohrs and Chevalier focused on the acoustic characterization of road surfaces used within the project, providing detailed insight into pavement-related parameters [40]. Böttcher et al. presented a vehicle-based measurement concept, describing sensor configurations and data acquisition strategies for large-scale tire–road noise monitoring [41]. In addition, Demetgül et al. highlighted the lack of large, diverse, and openly available datasets in this field and outlined data requirements and processing challenges for reliable tire–road noise analysis [6], [42]. These works collectively establish the experimental and data-related foundations upon which the present study builds. While these studies primarily addressed road characterization, measurement infrastructure, and data requirements, the present work focuses on condition-aware data-driven estimation of tire–road noise under limited-data conditions, with emphasis on generalization and realistic validation.

Overall, the literature shows a clear evolution in tire–road noise modeling. While hybrid and physics-informed models have shown strong performance in specific scenarios, purely data-driven approaches with physically meaningful inputs and outputs remain highly relevant for practical applications. In particular, AI-based models are able to learn complex nonlinear relationships directly from data. However, most existing studies are limited in scope and do not sufficiently address robustness across varying operating and environmental conditions. This highlights the need for data-driven models that can maintain stable performance across varying operating conditions while maintaining physical interpretability through appropriate signal representations and evaluation metrics.

In addition, many tire–road noise studies are conducted with relatively small datasets, which increases the risk of overfitting and unintended data leakage. However, these issues are rarely discussed explicitly in the literature. To mitigate these risks and improve model stability, ensemble learning strategies may provide important advantages. Furthermore, performance consistency across different conditions—such as tire type, road surface, vehicle, speed, and acceleration should be systematically evaluated using leave-one-group-out (LOGO) validation schemes. In this context, jointly estimating OBSI and tire cavity noise within a multi-task learning framework is particularly relevant, as these noise sources are physically related and allow shared representations to be learned, enabling information sharing between the two prediction tasks under limited-data conditions. In contrast to these studies, the present work focuses on condition-aware joint estimation of OBSI and tire-cavity noise from heterogeneous real-vehicle measurements and explicitly evaluates generalization to unseen tires, vehicles, speeds, and acceleration conditions. The methodological contribution therefore lies in the integration of these elements under limited-data conditions rather than in the individual learning algorithms themselves.

In this study, robustness is evaluated in terms of maintaining stable prediction performance across different tires, vehicles, speeds, acceleration levels, and multi-sensor operating conditions under limited-data scenarios. The main contributions of this study are as follows:

- A condition-aware data-driven framework for tire-road noise estimation under limited-data conditions.
- A multi-scale feature extraction strategy combining different temporal resolutions.
- A multi-task learning approach for the joint estimation of OBSI and tire cavity noise.
- A LOGO-based evaluation framework for assessing generalization to held-out operational conditions.
- An ensemble learning strategy that improves robustness and generalization across different tires, vehicles, speeds, and acceleration scenarios.

II. LITERATURE OVERVIEW

As shown in Table 1, most existing studies rely on a single noise-related signal, typically OBSI or tire cavity noise, sometimes combined with basic operating variables such as vehicle speed. The joint use of multiple noise sources together with vehicle-level information remains relatively limited. Signal processing approaches are mainly based on FFT, PSD, and 1/3-octave band analysis, while time–frequency methods are only used in specific applications. Similarly, feature extraction is often limited to handcrafted spectral features or dimensionality reduction techniques, with relatively little attention given to feature fusion across different data sources. From a modeling perspective, classical regression methods, SVMs, and individual neural network models are the most commonly adopted approaches, whereas ensemble-based methods have received comparatively less attention. Furthermore, although several studies investigate different tires, vehicles, or road surfaces, relatively few explicitly evaluate model performance under unseen operating conditions. As a result, the reported performance may not always reflect the challenges encountered in real-world applications where operating conditions vary significantly. These observations highlight the need for more robust frameworks capable of combining heterogeneous data sources while maintaining good generalization across different scenarios.

In this study, data were collected from four different vehicles operating under varying speeds, accelerations, tire types, and road surfaces using a sensor fusion setup compliant with relevant standards and CAN bus signals. In addition to vehicle dynamics data, On-Board Sound Intensity (OBSI) and tire cavity noise were recorded as raw acoustic signals to capture noise generation mechanisms close to the source.

TABLE 1. Literature overview.

	Sensors/Data	Signal Processing	Feature Extraction, Selection	AI Algorithm
[15]	OBSI	FFT	Statistical techniques	PCR, OLS
[43]	OBSI, Speed	SPL 1/3 OCT	-------------	SVM, NN
[35]	OBSI, PLP	-------------	Statistic model	Correlation Analysis
[38]	OBSI, PL, OS	FFT, STFT, velocity spectrum, Narrowband, 1/3 Octave Band	-------------	NN, Multitask
[11]	OBSI/Tread Pattern, Tire Features	1/3 Octave Band	Pixel-based method	SVM, RVM, NN, CNN
[36]	OBSI	FGM	-------------	Linear Regression, Regression Analysis
[9,29]	OBSI, CTWIST laser scanning, optical sensor	FFT, Power Spectrum	Gaussian curve fitting	NN
[44]	Tire Cavity/Different Roads	-------------	PCA	-------------
[24]	Tire Cavity/two tires, roads	SPL 1/3 OCT	-------------	Multiple Linear regression
[45]	Tire Cavity/Different roads	PSD	LDA, MANOVA	SVM
[46]	Tire Cavity/Different roads	SPL, PSD	-------------	NN
This study	Tire Cavity+OBSI+Vehicle CAN bus, Tire and Vehicle Features	SPL, MFCC	Statistical properties	Ensemble Learning, Multitask

The multi-scale strategy is based on multi-sensor fusion, combining time-series signals and static features to better represent the dynamic and nonlinear nature of tire–road interactions. A multi-task learning formulation was employed to jointly estimate OBSI and tire cavity noise, allowing shared representations to be learned from physically related noise sources and improving data efficiency. To further enhance generalization capability, an ensemble learning framework was applied, integrating multiple algorithms to reduce model variance and improve performance consistency across different operating conditions.

To prevent data leakage and ensure realistic performance evaluation, a Leave-One-Group-Out (LOGO) validation scheme was used. In each iteration, all samples corresponding to a specific driving condition (e.g., a given speed or acceleration scenario) were used exclusively as test data, while the remaining data were used for training. Final performance metrics were obtained by averaging results across independent validation trials, enabling a systematic assessment of model behavior under previously unseen operational conditions.

Overall, the proposed methodology addresses several limitations of existing tyre–road noise prediction studies, including the use of single sensing modalities, limited integration of heterogeneous data sources, and insufficient evaluation under unseen operating conditions. By combining multi-sensor data, multi-task learning, ensemble models, and condition-aware validation, the proposed framework aims to improve both robustness and generalization under realistic operating conditions.

III. METHODOLOGY

As shown in Fig. 1, the experimental campaign was conducted using multiple instrumented vehicles, different types of tires, and both ISO-compliant and non-ISO road surfaces. The experimental campaign was conducted using multiple instrumented vehicles, such as an Audi Q8 e-tron, a Volkswagen ID.4, a Porsche Taycan, and a Volkswagen e-Golf, all equipped with a comprehensive sensor system for tire–road noise acquisition.

FIGURE 1. All experimental conditions.

Several tire types with different designs and dimensions were tested, including Continental PremiumContact 6AO, Continental EcoContact 6Q, Hankook Ventus S1 evo3, Pirelli P Zero R, and BF Goodrich SRTT. Measurements were carried out on both ISO 10844-compliant asphalt and non-ISO asphalt road surfaces, allowing the analysis of tire–road noise under standardized conditions as well as more realistic road scenarios [40].

The vehicles were driven at speeds of 45 km/h, 80 km/h, and 100 km/h, and additional acceleration tests were conducted at 50 km/h with three levels of longitudinal acceleration (1, 2, and 3 m/s^2) to analyze dynamic effects on tire–road interaction [41]. For a detailed description of the measurement concept, sensor configuration, road surface characterization, and data collection procedures used within the Tire Road Noise project, the reader is referred to [6], [40],

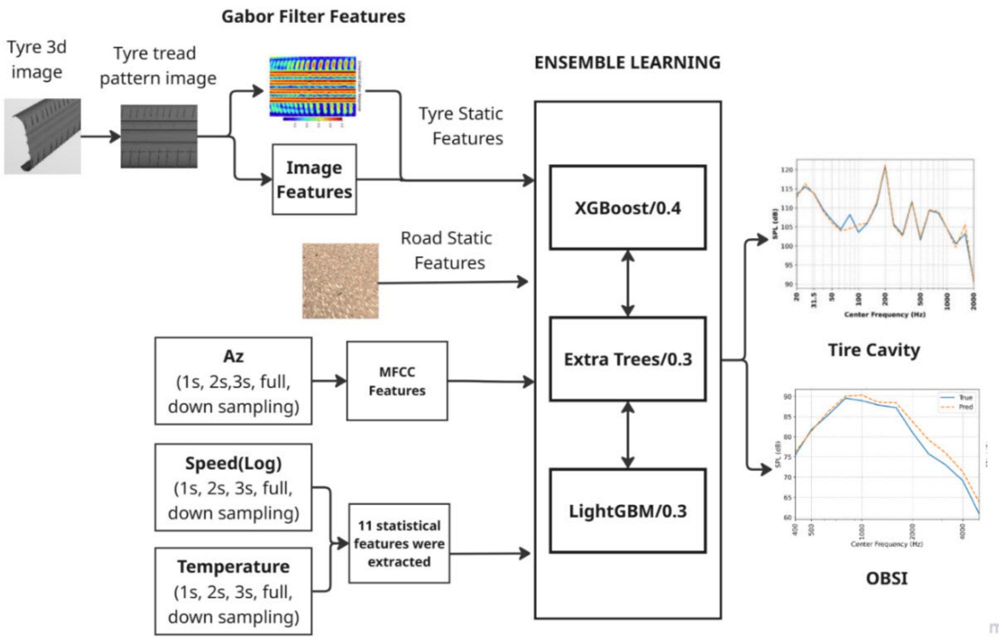

FIGURE 2. Multi-scale feature extraction and prediction framework.

[41], [42]. These studies provide comprehensive background information and complement the methodological focus of the present work. Although the overall Tire Road Noise (mFUND) project includes numerous sensors such as tire cavity microphones, roadside microphone arrays, and thermal cameras, this study focuses on a selected subset of signals.

Specifically, data from the vehicle CAN bus (speed, longitudinal acceleration (Ax), vertical acceleration (Az), and temperature) and the On-Board Sound Intensity (OBSI) lead microphones were used for analysis. This selection enables condition-aware tire–road noise prediction by combining informative and consistently available data sources while maintaining balanced model complexity. For the acceleration signals, 13 MFCC coefficients were extracted separately from the longitudinal (Ax) and vertical (Az) acceleration components and averaged over the temporal frames, resulting in 26 acceleration-related MFCC features in total. The pipeline used in the study is shown in Fig 2.

Due to limited data availability, a multi-scale strategy was adopted to improve feature diversity and enhance the reliability of the analysis. The dataset consisted of approximately 200 independent measurement recording (samples) collected under 4 vehicles, 6 tire models, 3 speed conditions, 3 acceleration conditions, and 2 road surface types. To better capture both short-term and long-term temporal dynamics, each measurement was processed using a multi-scale segmentation strategy with window lengths of 1 s, 2 s, and 3 s. These segments were used to extract complementary feature representations rather than to create independent experimental conditions. Accordingly, the multi-scale segments are not interpreted as additional independent measurements, but as correlated temporal observations derived from the original recordings. The primary role of this strategy is to increase the number of usable temporal observations under the limited-data setting while representing the measured signals at different temporal resolutions. Furthermore, all segments originating from the same measurement recording were assigned to the same LOGO fold, ensuring that segments from the same original measurement never appeared in both the training and test folds and thereby preventing information leakage.

The procedure summarized in Table 2 defines the complete workflow used for calculating the SPL based features in accordance with acoustic measurement standards. The analysis follows the general framework of ISO for sound intensity measurement, which establishes the computation of directional acoustic energy using paired microphone signals. The frequency-domain representation and band partitioning were designed according to the ISO one-third-octave standard, defining 12 one-third-octave center frequencies between 400 Hz and 5000 Hz, covering the dominant tire–road-noise frequency range considered in this study.

First, two simultaneously measured microphone signals (p_1 and p_2) are band-pass filtered to eliminate unwanted frequencies. The instantaneous intensity, I(t), is then computed according to the standardized pressure-difference formulation, which considers air density (ρ), sound speed (c), and microphone spacing (Δr). The resulting signal is transformed into the frequency domain via FFT, and power values are integrated within the ISO-defined band limits to determine the energy content of each band. Each band's sound intensity level is calculated using a reference intensity

TABLE 2. Computation of OBSI Sound Pressure Levels (SPL).

Step	Operation	Description
1	Band-pass filtering	Apply a band-pass filter to p_1 and p_2 over the selected frequency range of **400–5000 Hz**.
2	Sound intensity estimation	Estimate the sound intensity from the two microphone pressure signals p_1 and p_2 using the two-microphone pressure-gradient (p-p) method.
3	FFT transformation	Apply FFT using a Hann window to obtain the frequency-domain representation for spectral analysis.
4	Frequency bands	Define one-third-octave center frequencies from **400 to 5000 Hz**, resulting in **12 frequency bands**.
5	Band limits	Determine the lower and upper frequency limits of each one-third-octave band.
6	Band integration	Integrate the sound intensity spectrum within each one-third-octave frequency band.
7	SIL computation	Calculate the sound intensity level (SIL) for each band using the reference intensity $\mathbf{I_0 = 10^{-12}}$ **W/m²**.
8	Overall SPL computation	Calculate the overall A-weighted sound pressure level (SPL) from the one-third-octave band levels using the corresponding A-weighting corrections.
9	Feature extraction	Extract the **12 one-third-octave SIL values** as acoustic features for subsequent analysis.
10	ML integration	Use the extracted acoustic features as inputs to the machine-learning model.

of 10^{-12} W/m^2, yielding 12 SIL values across the full frequency range.

These SIL values describe the directional acoustic energy distribution radiated by the tire–road interface and are used as physical, frequency-domain input features for data-driven tire–road noise prediction. The overall methodology follows standardized acoustic measurement principles and conceptually aligns with established tire–road noise testing procedures. This supports physical validity and reproducibility while extending traditional acoustic analysis toward data-driven modeling. This ensures physical validity and reproducibility while extending traditional acoustic analysis toward data-driven modeling.

The proposed workflow demonstrates how multi-scale time-domain signals are transformed into predictive features for SIL and SPL estimation. Each raw signal (e.g., speed, temperature, acceleration, and tire-related data(tire width, aspect ratio, rim diameter, label noise level, tread width, sidewall height, stiffness index, tire mass, and rolling resistance coefficient) is segmented into time windows of 1, 2, and 3 seconds to capture both short-term and long-term dynamic behavior. From each segment, eleven statistical descriptors—such as mean, standard deviation, minimum, maximum, interquartile range, and higher-order moments—are extracted to characterize the signal variability and stability (Fig 2). Subsequently, five regression-based machine learning algorithms were employed to predict the one-third-octave SPL spectra of tire cavity noise (20–2000 Hz) and the one-third-octave SIL spectra of OBSI (400–5000 Hz).

For regression-type prediction tasks, several common machine learning models can be used, including Ridge Regression [47], Extra Trees [48], Random Forest [49], XGBoost and Multi-Layer Perceptron (MLP) [50].

Ridge Regression is a linear model that applies L2 regularization to reduce coefficient magnitudes and improve stability when features are correlated. Random Forest and Extra Trees are tree-based ensemble methods that combine many decision trees to improve robustness and reduce overfitting, with Extra Trees introducing additional randomness in tree construction. XGBoost is also a tree-based ensemble model that builds decision trees sequentially, but, as a gradient boosting method, it fits each new tree to the residual errors of the previous ensemble using gradient-based optimization. MLP is a neural network model that can capture nonlinear relationships by learning multiple hidden representations from the input data. However, these models are often insufficient when used individually, as they capture different aspects of the data. Linear models are effective for describing global trends, while nonlinear models better represent complex interactions. To leverage the complementary strengths of these approaches, ensemble learning is required, allowing linear and nonlinear behaviors to be combined within a unified and more robust prediction framework.

In addition to dynamic acoustic and vehicle signals, static tire-related features were extracted from 3D tire tread scans. As illustrated in Fig. 3, the raw 3D tire scans were first converted into height maps representing the tread surface structure. The 3D STL scans were not directly used as model inputs; instead, each STL surface was converted into a two-dimensional height map using linear interpolation on a regular grid of 128 lateral $\times$ 2048 circumferential points. Subsequently, two complementary analysis approaches were applied: Power Spectral Density (PSD)-based analysis and Gabor filter-based texture analysis. The PSD analysis was used to characterize frequency-domain tread properties such as dominant frequency, spectral entropy, autocorrelation decay, and PSD slope, while the Gabor-based analysis captured directional and texture-related characteristics including dominant orientation, anisotropy, and multi-scale energy distributions. For the Gabor analysis, the height maps were normalized to the range [0,1] and processed using eight orientations between 0 and 180 degrees at 22.5-degree increments and five wavelengths of 5, 20, 35, 60, and 75 pixels. For each wavelength, the Gaussian standard deviation was set to 0.56 times the wavelength, with an adaptive odd kernel size of approximately six times the standard deviation. The spatial aspect ratio was set to 0.5 and the phase offset to 0. Thus, image processing is used in this framework specifically for extracting tire-tread characteristics from 3D scans rather than as the primary prediction modality. The resulting static tire descriptors were integrated with dynamic multi-sensor signals within the proposed data-driven framework.

A. INDIVIDUAL MODELS

Before investigating ensemble learning, the models need to be evaluated individually as a reference. The performance of the regression models Ridge Regression, Extra Trees, Random Forest, XGBoost, and MLP are evaluated in a first experiment with three goals:

1) MULTI-TASK VS SINGLE-TASK

Two related prediction targets are considered, namely OBSI and tire-cavity predictions, and investigate both single-task

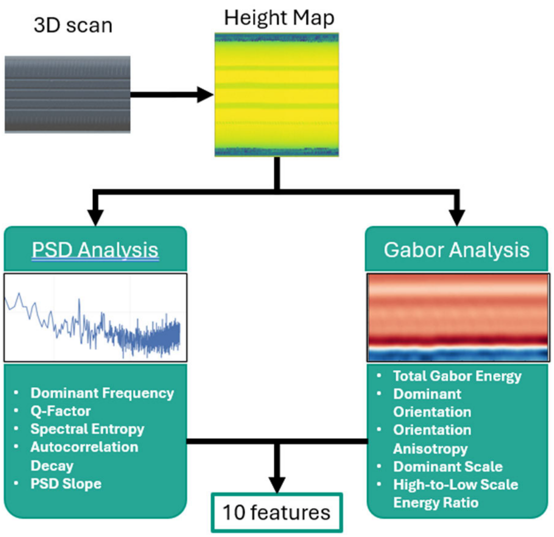

FIGURE 3. Static tire feature extraction pipeline based on PSD and Gabor analysis from 3D tire tread scans.

and multi-task learning settings. In the single-task setting, separate models are trained independently for each target. In the multi-task setting, a joint model is trained to predict both targets simultaneously. This setup allows the model to exploit potential correlations between the two targets. To ensure a fair comparison, both approaches use the same input features, data splits, and evaluation protocol. Performance is evaluated separately for each target, and results are compared between single-task and multi-task models to assess whether joint learning provides a benefit. The multi-task setup of the MLP involves two shared hidden layers (sizes 256 and 128) followed by task-specific heads (sizes 64). Its corresponding single-task setup has only one head of size 64, making the multi-task setup slightly more computationally costly, having more parameters. Extra Trees and Random Forest use the same parameters in the multi-task and single-task setup. XGBoost and Ridge Regression do not support multi-output prediction natively in the implementation used; therefore, separate target-specific models were trained. Models' hyperparameters were selected using a limited grid search.

2) FEATURE IMPORTANCE

To justify the feature selection, a feature importance evaluation is performed. The feature importance is determined by calculating each model's SHAP values. SHAP values are a method for interpreting machine learning models by assigning each feature a contribution to an individual prediction [50]. They quantify how much each feature increases or decreases the model's output compared to a baseline prediction. Global feature importance was obtained by averaging absolute SHAP values across all background samples and folds. To produce a reliable result, SHAP values were computed using the full training set as background samples.

3) GROUP SPECIFIC

Model performance may vary when presented with data under a new condition. To identify these potential performance limitations, a group-wise evaluation is conducted by observing the models' performance on the held-out LOGO test set. The LOGO validation strategy was specifically adopted to evaluate robustness under previously unseen operational conditions while minimizing the risk of data leakage between training and test sets.

In total, 16 distinct groups are used as test sets. A breakdown of model performance across these groups provides insight into the strengths and weaknesses of the individual classical models and highlights condition-specific performance variations.

B. ENSEMBLE LEARNING

Ensemble learning was adopted to improve robustness and generalization under limited-data conditions. The group-specific analysis demonstrated that no individual model consistently achieved the best performance across all tires, vehicles, speeds, and acceleration conditions. The effectiveness of this ensemble strategy is quantitatively assessed by comparing the group-wise performance of the individual models (Figs. 8–9 and Figs. 13–14) with the corresponding ensemble results (Tables 3–5 and Tables 7–9). While some algorithms performed better for specific groups, their performance deteriorated under other operating scenarios. To exploit the complementary strengths of different learning algorithms, an ensemble framework was employed. The final prediction was obtained by combining the outputs of the best-performing individual models using weighted averaging. This approach reduces model variance and provides more stable prediction performance across previously unseen conditions.

IV. RESULTS

The models Ridge Regression, Extra Trees, Random Forest, XGBoost, and MLP were tested individually and in an ensemble. The results of these two experiments are presented in the following.

A. INDIVIDUAL MODELS RESULTS

1) MULTI-TASK VS SINGLE-TASK

The performance comparison between single-task and multi-task models across all algorithms is shown in Fig. 4-6. Performance is assessed separately for OBSI and tire-cavity predictions using both MAE and RMSE, which have been averaged across all LOGO folds. The primary motivation for multi-task learning is therefore to enable information sharing between the physically related OBSI and tire-cavity tasks through shared representations, rather than to guarantee higher prediction accuracy.

The errors are presented in Fig 4 using only tire groups, which shows RMSE and MAE as stacked bars. The comparison shows that the impact of joint learning is strongly model-dependent. For Random Forest and Extra Trees, the differences between single-task and multi-task settings are minimal, indicating that these models do not meaningfully benefit from shared learning.

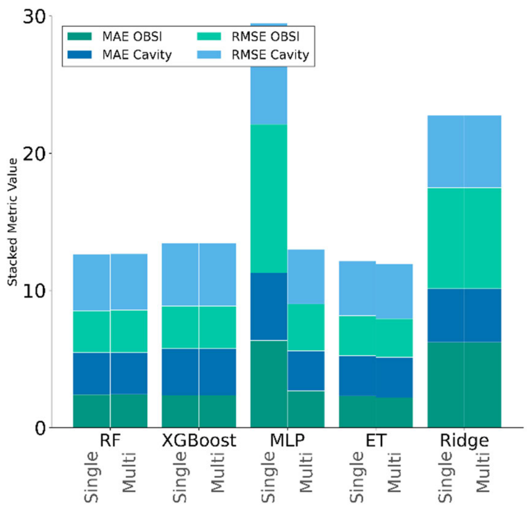

FIGURE 4. **Error comparison of multi-task vs single-task models using only tire groups.**

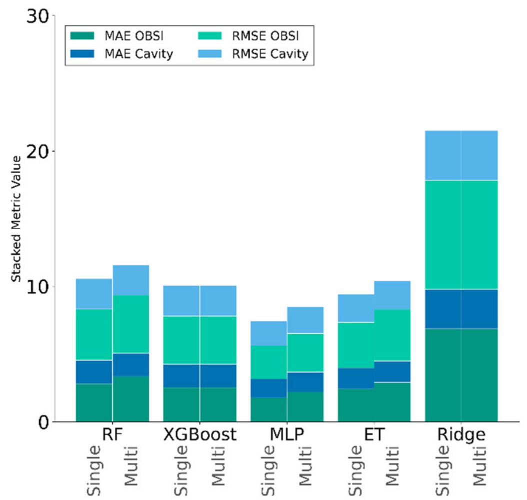

FIGURE 5. **Error comparison of multi-task vs single-task models using only speed groups.**

In contrast, the MLP exhibits a clear improvement in the multi-task setting, where the stacked error is lower than in the single-task configuration across both MAE and RMSE for OBSI and tire cavity predictions. This suggests that the shared representation enables the model to exploit common structure between the tasks, leading to better generalization. Overall, the results indicate that multi-task learning is beneficial primarily when the model architecture is capable of learning shared representations, as demonstrated by the MLP. In contrast, Figure 5 shows that, for speed-based grouping, the single-task models generally perform better. The overall RMSE and MAE are lower than in Figure 4 except for Ridge regression. Meanwhile, in Figure 6 the vehicle groups seem to show a benefit for the multi-task model. Notably, the multi-task model is better for Extra Trees and MLP.

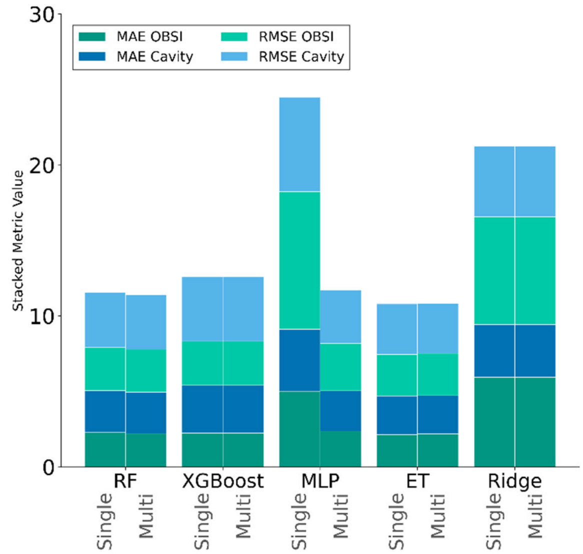

FIGURE 6. **Error comparison of multi-task vs single-task models using only vehicle groups.**

2) FEATURE IMPORTANCE

Following the methodology, feature importance was evaluated using SHAP-based importance values. Additionally, a ranking score is assigned to ensure consistent assessment across different learning algorithms. While SHAP values provide a theoretically grounded measure of feature contribution within each model, the additional ranking-based aggregation enables evaluation across models with potentially different importance scales and distributions. The average importance was derived from SHAP values computed for each model by taking the mean of the absolute SHAP values across all samples, folds and models. A rank score was computed to provide a complementary perspective. For each of the five evaluated models, features were first ranked based on their individual importance values, with rank 1 assigned to the most important feature. These ranks were then summed across all models to obtain an aggregate ranking score per feature. To ensure interpretability, the aggregated scores were inverted such that higher values correspond to higher importance. This approach emphasizes consistency across models, highlighting features that are consistently ranked highly even if their absolute importance values differ.

The feature importance analysis shown in Fig. 7 illustrates the average importance of feature categories across five machine learning algorithms: Random Forest, XGBoost, MLP, Extra Trees, and Ridge Regression.

It reveals that speed is by far the most influential predictor, with an average importance of 55.9%, substantially higher than all other features. The rank score indicates how

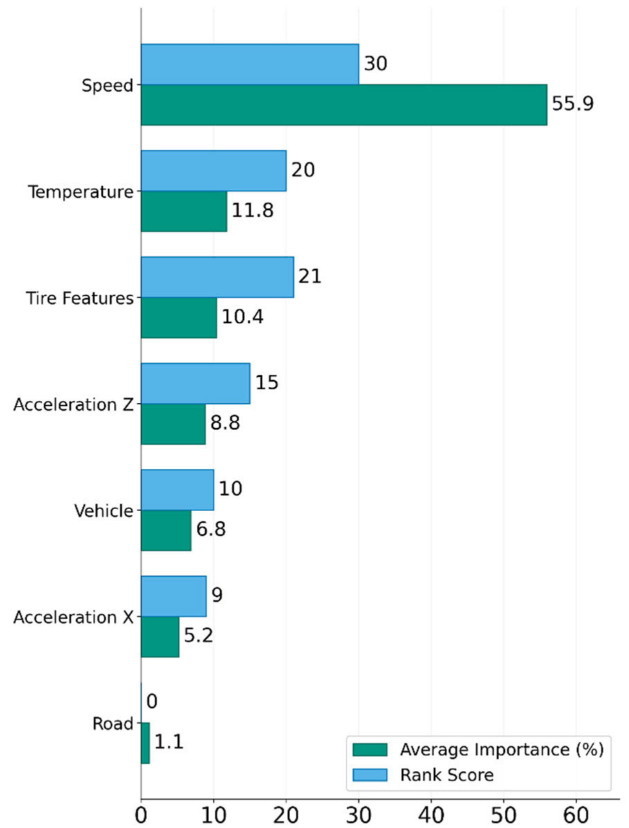

FIGURE 7. Importance of feature categories using all groups, averaged over models.

OBSI R^2

	RF Single	RF Multi	XGBoost Multi	MLP Single	MLP Multi	ET Single	ET Multi	Ridge Multi
1 m/s²	0.932	0.923	0.946	0.971	0.937	0.953	0.946	0.506
2 m/s²	0.950	0.951	0.944	0.940	0.937	0.947	0.932	0.731
3 m/s²	0.766	0.730	0.777	0.792	0.810	0.788	0.746	0.644
45 km/h	0.668	0.403	0.882	0.803	0.719	0.888	0.637	-1.031
80 km/h	0.932	0.896	0.866	0.920	0.888	0.915	0.932	0.291
100 km/h	0.559	0.543	0.547	0.947	0.921	0.568	0.565	-0.400
Mean	0.801	0.741	0.827	0.896	0.869	0.843	0.793	0.124

0.0 0.2 0.4 0.6 0.8 1.0
R^2 performance, 0=worst, 1=best

FIGURE 8. OBSI prediction performance (R^2) across speed and acceleration groups.

consistently each feature was identified as important across the applied feature-importance methods. Speed dominates both measures, consistent with its strong influence on tire–road noise generation, while tire-related features also show consistently high relevance. The next most relevant features are temperature and tire features, followed by acc. Z and vehicle-related features. The low importance of road type should be interpreted cautiously, as it may reflect the limited diversity of road surfaces in the dataset or correlations with other explanatory variables rather than the intrinsic physical importance of road type. Notably, the lateral acceleration (acc. X) has a smaller impact than the vertical (acc. Z).

3) GROUP SPECIFIC

Figures 8 and 9 present the group-wise OBSI prediction performance (R^2) obtained using leave-one-group-out evaluation across speed/acceleration and vehicle groups, respectively. Overall, the nonlinear machine learning models achieve strong predictive performance across most test groups, with average R^2 values generally exceeding 0.80. The acceleration-based groups (1 m/s^2 and 2 m/s^2) exhibit consistently high prediction accuracy, whereas the 45 km/h and 100 km/h groups represent more challenging scenarios and lead to noticeable performance degradation for several models. A similar trend can be observed across vehicle groups, where the VW ID.4 yields the most stable results, while the Taycan and VW e-Golf groups prove more difficult to predict. Among the evaluated approaches, MLP achieves the highest average performance across the speed and acceleration groups, whereas Random Forest, XGBoost, and Extra Trees demonstrate more stable behavior across different vehicle types. In contrast, Ridge Regression consistently exhibits the weakest performance and the poorest generalization capability. These findings highlight both the effectiveness of nonlinear learning methods for OBSI prediction and the influence of operating conditions and vehicle characteristics on model robustness. The group-wise OBSI prediction results for the tire groups are provided in Appendix (Figure 13). The observed trends are largely consistent with those reported for the speed, acceleration, and vehicle groups, supporting the observed robustness of nonlinear learning approaches across the evaluated tire types.

OBSI R^2

	Single	Multi	Multi	Single	Multi	Single	Multi	Multi
Taycan	0.888	0.881	0.861	-4.983	0.758	0.879	0.895	0.229
VW ID.4	0.932	0.925	0.929	0.934	0.937	0.941	0.941	0.554
VW e-Golf	0.784	0.811	0.822	0.752	0.756	0.813	0.834	0.348
Mean	0.868	0.872	0.871	-1.099	0.817	0.878	0.890	0.377

FIGURE 9. OBSI prediction performance (R^2) across vehicle groups.

A similar breakdown for the tire-cavity prediction task is provided in Appendix (Figure 14), where the R^2 performance is reported for each group and model. Overall, the observed trends are consistent with those reported for OBSI prediction. Random Forest and Extra Trees exhibit the most stable performance across most test groups, while XGBoost shows slightly greater variability. The P-Zero tire and Taycan vehicle groups represent the most challenging test scenarios, leading to substantially reduced performance for some models, particularly MLP and Ridge Regression. This condition-dependent degradation also explains why the MLP was not included in the final ensemble, which instead uses models exhibiting more stable and complementary performance across the LOGO groups. In general, the tree-based ensemble methods demonstrate the strongest robustness and generalization capability across different operating conditions, tire types, and vehicle categories.

It should be noted that each learning algorithm exhibits its own strengths and weaknesses. While some models perform exceptionally well for specific groups or operating conditions, none of the individual algorithms consistently achieves the best performance across all categories. This observation highlights the complementary nature of the evaluated models and suggests that combining multiple learning approaches through an ensemble framework can improve robustness and generalization.

4) ENSEMBLE LEARNING

The proposed ensemble framework significantly improved OBSI prediction performance compared with the best individual model. While the MLP achieved a mean R^2 of approximately 0.87 across the speed and acceleration groups (Figure 8), the ensemble increased this value to approximately 0.93. At the same time, both MAE and RMSE were noticeably reduced (Table 6). The most significant improvements were observed in the challenging 45 km/h, 80 km/h, and 3 m/s^2 groups, highlighting the ensemble approach's ability to enhance robustness and generalization.

To quantify the contribution of ensemble learning, Table 3 compares the mean R^2 of the best-performing individual model with the corresponding ensemble result for each LOGO grouping and prediction target. As summarized in Table 3, the ensemble outperformed the best individual model in five of the six evaluated settings. The largest improvements were obtained for tire-cavity prediction under vehicle and tire LOGO evaluation, while substantial improvements were also observed for OBSI prediction. For tire-cavity prediction under speed and acceleration conditions, the best individual model already achieved high performance, and the ensemble maintained a comparable R^2.

A similar improvement was observed for the vehicle-based evaluation. As shown in Figure 9, the best-performing individual model, Extra Trees, achieved a mean R^2 value of approximately 0.89 across the vehicle groups. Using the proposed ensemble framework, the mean R^2 increased to approximately 0.95, accompanied by further reductions in both MAE and RMSE (Table 4).

TABLE 3. Comparison of best individual and ensemble model performance.

Target	LOGO Group	Best Model	Individual R^2	Ensemble R^2
OBSI	Speed & Acc.	ET	0.89	0.95
OBSI	Vehicle	ET	0.89	0.95
OBSI	Tire	ET	0.91	0.95
Tire-Cavity	Speed & Acc.	MLP	0.95	0.93
Tire-Cavity	Vehicle	ET	0.73	0.86
Tire-Cavity	Tire	ET	0.80	0.90

Table 5 presents the performance of the proposed ensemble model across different tire groups. Compared with the best-performing individual model, Extra Trees (mean $R^2 \approx 0.92$), the ensemble framework achieved a notable improvement, increasing the overall mean R^2 to 0.956. In addition, both MAE and RMSE were reduced, indicating improved prediction accuracy and robustness.

TABLE 4. OBSI ensemble learning model prediction performance across speed and acceleration groups.

Vehicle	R^2	MAE (dB)	RMSE (dB)
audiq8	0.969	1.416	1.793
porsche	0.905	2.198	2.750
vwegolf	0.919	2.049	2.496
vwid4	0.958	1.769	2.120
OverallMean	0.953	1.751	2.172

TABLE 5. OBSI ensemble learning model prediction performance across vehicle groups.

Tire Model	R^2	MAE (dB)	RMSE (dB)
Eco	0.979	1.204	1.447
PZe	0.905	2.198	2.750
Ven	0.961	1.623	2.005
Sum	0.919	2.049	2.490
Rain	0.960	1.764	2.110
Pre	0.969	1.365	1.762
Overall Mean	0.956	1.679	2.099

The largest gains were observed for the more challenging tire groups, particularly P-Zero, where individual models previously exhibited reduced generalization capability. Overall,

TABLE 6. OBSI ensemble learning model prediction performance across TIRE groups.

Acceleration	R2	MAE (dB)	RMSE (dB)
1 m/s²	0.936	1.986	2.543
2 m/s²	0.984	0.943	1.180
3 m/s²	0.983	0.890	1.188
Overall Mean	0.967	1.279	1.766
Speed			
45 km/h	0.893	2.542	3.130
80 km/h	0.971	1.165	1.547
100 km/h	0.922	2.107	2.560
Overall Mean	0.937	1.944	2.507

the results demonstrate that combining multiple tree-based learning algorithms enables the ensemble model to exploit their complementary strengths and achieve more reliable predictions across different tire types.

The effectiveness of the proposed ensemble framework becomes evident when compared with the individual learning algorithms presented in Appendix (Figure 14). Among the standalone models, Extra Trees achieved the highest overall tire-cavity prediction performance with a mean R^2 value of approximately 0.83, while Random Forest achieved a mean R^2 of approximately 0.80. However, several challenging groups, including P-Zero and Taycan, resulted in substantial performance degradation for some algorithms.

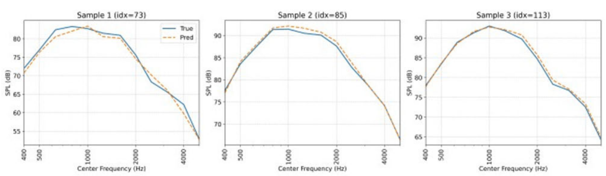

FIGURE 10. OBSI prediction performance (R^2) across acceleration groups.

Appendix (Tables 8–A4) summarizes the tire-cavity prediction performance of the proposed ensemble model across speed, acceleration, vehicle, and tire groups. Overall, the model achieved strong predictive accuracy, with mean R^2 values of 0.907 for speed-based evaluation, 0.964 for acceleration-based evaluation, 0.869 for vehicle-based evaluation, and 0.906 for tire-based evaluation. The results indicate that acceleration groups were generally easier to predict than speed groups, while some variability was observed across different vehicle and tire categories. Nevertheless, the consistently high R^2 values demonstrate the robustness and generalization capability of the proposed ensemble framework across diverse operating conditions.

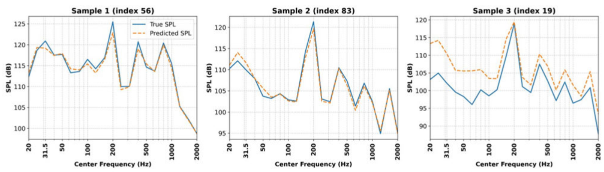

FIGURE 11. Tire-Cavity prediction performance (R^2) across acceleration groups.

Figures 10–12 provide a qualitative assessment of the proposed ensemble model. The example spectra in Figures 10 and 11 show close agreement between the predicted and measured SPL profiles for both OBSI and tire-cavity noise, indicating that the model successfully captures the main spectral characteristics of the acoustic signals. The frequency-dependent prediction behavior also provides physical insight into the model performance. The higher accuracy observed in the 400–5000 Hz range coincides with the frequency region in which important tire–road interaction mechanisms, including tread-related vibration and aerodynamic effects such as air pumping, contribute to the measured noise.

Furthermore, the predicted-versus-measured comparisons in Figure 12 demonstrate a strong linear relationship and high prediction accuracy, with R^2 values exceeding 0.96 for both targets. These results further validate the robustness and generalization capability of the proposed ensemble framework.

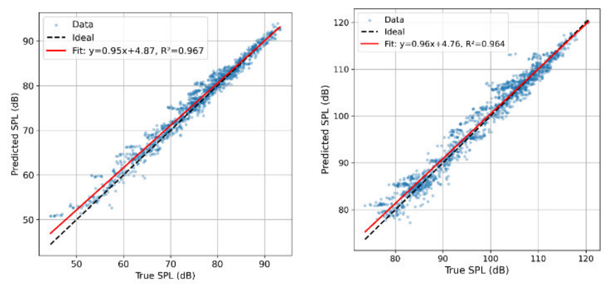

FIGURE 12. Predicted versus measured SPL values for OBSI (left) and tire cavity noise (right) using the proposed ensemble framework.

V. CONCLUSION

This study proposed a data-driven framework with physically meaningful signal representations for tire–road noise prediction, explicitly addressing several key challenges commonly encountered in the literature. The main conclusions can be summarized as follows:

Physically meaningful SPL and SIL-based representation: An SPL and SIL-based, one-third-octave representation was adopted as an alternative to conventional overall sound level metrics to better capture frequency-dependent acoustic energy radiated by the tire–road interface, particularly in mid-frequency bands relevant to tire–road noise generation.

Performance stability under limited-data conditions: The proposed framework was specifically designed for scenarios with limited data availability. By combining multi-scale segmentation, statistical feature extraction, and ensemble learning, the approach helps reduce overfitting risk and improves model stability under small-sample conditions.

Multi-sensor data fusion: Time-series and static features derived from multiple sensors, including acceleration, temperature, and vehicle speed, were jointly exploited to represent the dynamic and nonlinear nature of tire–road interactions.

Multi-task learning for related noise sources: OBSI and tire cavity noise were jointly estimated within a multi-task learning formulation, allowing shared representations to be learned from physically related acoustic sources and improving data efficiency compared to single-task modeling.

Data-leakage-aware evaluation: To ensure realistic performance evaluation, a Leave-One-Group-Out (LOGO) validation strategy was employed, explicitly preventing data leakage across driving conditions such as tire type, road surface, speed, and acceleration.

Robustness across diverse operating conditions: A comprehensive experimental dataset was collected, covering multiple tires, road surfaces, vehicles, speeds, and accelerations. This enabled a systematic assessment of model behavior under previously unseen operational conditions.

Generalization behavior across tires and frequencies: While combining data from different tire types initially reduced prediction accuracy due to increased acoustic variability, the results highlight the importance of balanced datasets. Higher accuracy observed in the 400–5000 Hz range is consistent with dominant tire–road noise mechanisms and indicates consistent frequency-wise prediction behavior.

Overall, this study proposed a reproducible data-driven framework with physically meaningful signal representations for tire–road noise prediction under limited-data conditions. By combining multi-scale feature extraction, multi-task learning, ensemble learning, and LOGO-based validation, the proposed methodology demonstrated consistent prediction performance across the evaluated vehicles, tires, speeds, and acceleration scenarios while explicitly preventing information leakage. Although the experiments were conducted under a limited number of road surfaces and controlled measurement conditions, the proposed framework provides a solid foundation for future extensions toward larger datasets, additional sensing modalities, and real-time tire–road noise monitoring applications.

Although the proposed framework demonstrated stable performance across multiple vehicles, tires, speeds, and acceleration scenarios, the current experiments were conducted under a limited number of road surfaces and controlled measurement conditions. Therefore, the demonstrated robustness should be interpreted within the scope of the evaluated operational scenarios rather than as universal robustness for deployment under all real-world conditions. Extending the framework to a broader range of pavement types may introduce additional acoustic and texture variability, and its performance should therefore be re-evaluated on larger and more diverse datasets.

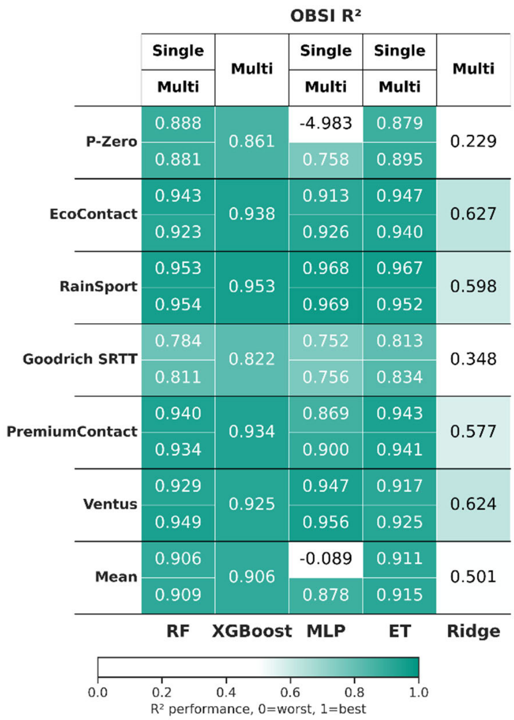

FIGURE 13. Group-wise OBSI prediction performance across tire groups.

TABLE 7. Ensemble tire-cavity prediction performance across speed and acceleration groups.

Test Group	R^2	MAE (dB)	RMSE (dB)
45 km/h	0.815	2.491	3.153
80km/h	0.963	1.464	1.979
100m/h	0.943	2.146	2.690
Overall Mean	0.907	2.033	2.607
1 m/s²	0.930	2.081	2.717
2 m/s²	0.962	1.111	1.494
3 m/s²	0.976	1.260	1.645
Overall Mean	0.964	1.484	1.952

TABLE 8. Ensemble tire-cavity prediction performance across vehicle groups.

Vehicle	R^2	MAE (dB)	RMSE (dB)
Audi Q8	0.822	2.760	3.557
Porsche Taycan	0.888	2.788	3.380
VW Golf	0.853	3.034	4.288
VW ID4	0.912	2.228	2.893
Overall Mean	0.869	2.703	3.529

FUTURE WORK

In future work, this project will be extended through large-scale data collection across Germany using a vehicle fleet

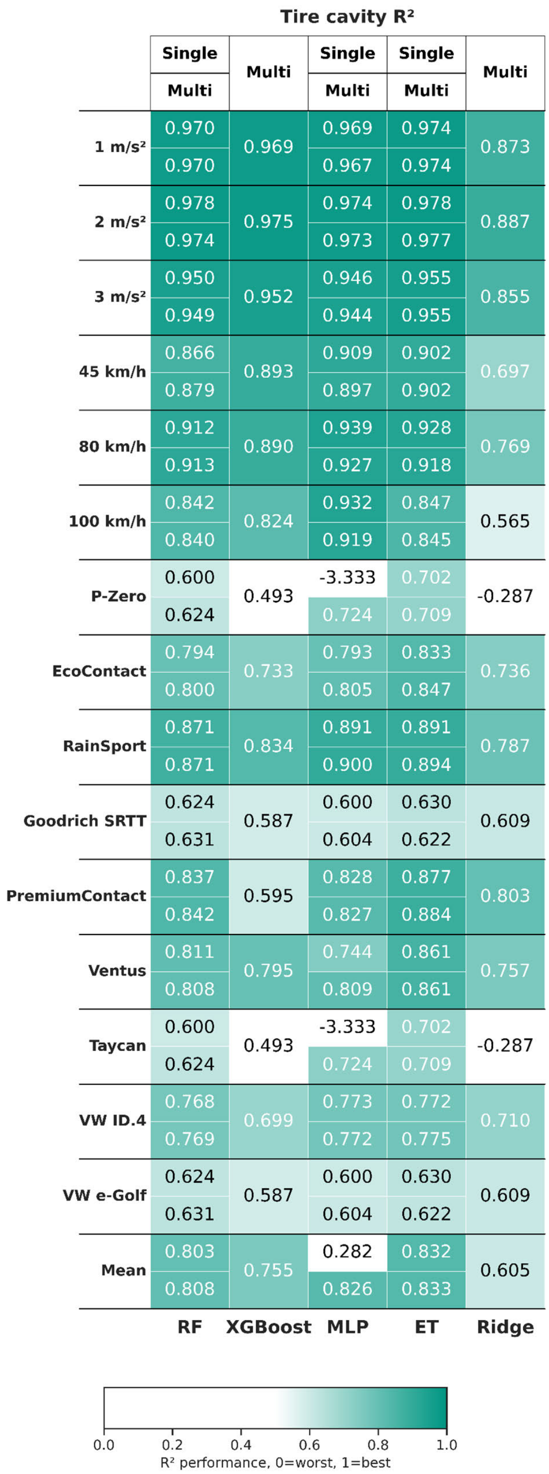

FIGURE 14. Group-wise tire-cavity prediction performance across speed, acceleration, vehicle, and tire groups.

in real driving conditions. The planned measurements will include many new tire types and road surfaces collected at more than ten different locations, which will significantly increase the size and diversity of the dataset. As more data becomes available, the current processing and modeling pipeline will be updated to handle the increased data volume and variability. With a larger and more diverse dataset, future work will also investigate deep-learning and physics-informed approaches under the same group-wise validation framework. Overall, fleet-based data collection will support better generalization and help move the proposed framework closer to real-world deployment.

As part of future work within the Tire Road Noise project, the collected multi-sensor dataset is planned to be made openly available to the research community. Providing open access to standardized tire–road noise data is expected to support reproducibility, facilitate benchmarking of data-driven methods, and foster further research on condition-aware noise estimation under varying operating conditions.

TABLE 9. Ensemble tire-cavity prediction performance across tire groups.

Tyre Model	R^2	MAE (dB)	RMSE (dB)
EcoContact 6 Q	0.937	2.263	2.800
P Zero R	0.888	2.788	3.380
Ventus S1 Evo 3	0.891	2.161	2.712
Summer SRTT	0.853	3.034	4.288
RainSport 5	0.936	1.962	2.415
PremiumContact 6	0.932	1.680	2.180
Overall Mean	0.906	2.315	2.962

APPENDIX

See Figures 13 and 14
See Tables 7, 8 and 9

ACKNOWLEDGMENT

With the mFUND funding program, the BMV has been supporting research and development projects relating to data-based digital innovations for Mobility 4.0 since 2016. The project funding is supplemented by active professional networking between stakeholders from politics, business, administration and research and the provision of open data on the Mobilithek. Further information can be found at www.mfund.de.

REFERENCES

[1] E. Murphy, W. Huang, J. Bessac, J. Wang, and R. Kotamarthi, "Joint modeling of wind speed and wind direction through a conditional approach," *Environmetrics*, vol. 36, no. 3, Apr. 2025, Art. no. e70011, doi: 10.1002/env.70011.

[2] *Burden of Disease From Environmental Noise: Quantification of Healthy Life Years Lost in Europe*, World Health Organization, Copenhagen, Denmark, 2011.

[3] S. A. Stansfeld and M. P. Matheson, "Noise pollution: Non-auditory effects on health," *Brit. Med. Bull.*, vol. 68, no. 1, pp. 243–257, Dec. 2003, doi: 10.1093/bmb/ldg033.

[4] J. Winroth, W. Kropp, C. Hoever, T. Beckenbauer, and M. Männel, "Investigating generation mechanisms of tyre/road noise by speed exponent analysis," *Appl. Acoust.*, vol. 115, pp. 101–108, Jan. 2017, doi: 10.1016/j.apacoust.2016.08.027.

[5] C. Ramos-Romero, C. Asensio, R. Moreno, and G. de Arcas, "Urban road surface discrimination by tire-road noise analysis and data clustering," *Sensors*, vol. 22, no. 24, p. 9686, Dec. 2022, doi: 10.3390/s22249686.

[6] M. Demetgul and S. Lazarova-Molnar, "Data-driven artificial intelligence applications for tyre-road-noise prediction and road condition monitoring: A review and future directions," *Measurement*, vol. 264, Mar. 2026, Art. no. 120203, doi: 10.1016/j.measurement.2025.120203.

[7] A. Kuijpers and G. Van Blokland, "Tyre/road noise models in the last two decades: A critical evaluation," in *Proc. INTER-NOISE NOISE-CON Congr. Conf.*, 2001, pp. 2494–2499.

[8] S. Mohammadi and A. Ohadi, "A novel approach to design quiet tires, based on multi-objective minimization of generated noise," *Appl. Acoust.*, vol. 175, Apr. 2021, Art. no. 107825, doi: 10.1016/j.apacoust.2020.107825.

[9] T. Li, R. Burdisso, and C. Sandu, ""The effects of tread patterns on tire pavement interaction noise," in *Proc. INTER-NOISE NOISE-CON Congr. Conf.*, 2016, pp. 208–219.

[10] R. E. Hayden, "Roadside noise from the interaction of a rolling tire with the road surface," *J. Acoust. Soc. Am.*, vol. 50, p. 113, Jun. 1971, doi: 10.1121/1.1977497.

[11] S. Mohammadi, A. Ohadi, and M. Irannejad-Parizi, "A comprehensive study on statistical prediction and reduction of tire/road noise," *J. Vib. Control*, vol. 28, nos. 19–20, pp. 2487–2501, Oct. 2022, doi: 10.1177/10775463211013184.

[12] M. Ohiduzzaman, O. Sirin, E. Kassem, and J. Rochat, "State-of-the-art review on sustainable design and construction of quieter pavements—Part 1: Traffic noise measurement and abatement techniques," *Sustainability*, vol. 8, no. 8, p. 742, Aug. 2016, doi: 10.3390/su8080742.

[13] G. Dubois, J. Cesbron, H. P. Yin, F. Anfosso-Lédée, and D. Duhamel, "Statistical estimation of low frequency tyre/road noise from numerical contact forces," *Appl. Acoust.*, vol. 74, no. 9, pp. 1085–1093, Sep. 2013, doi: 10.1016/j.apacoust.2013.03.011.

[14] S. Yang, Y. Wei, Z. Ye, H. Liu, B. Yang, W. Liu, and L. Wang, "Characterization and modeling of textured cement concrete pavement surfaces for tire-pavement noise prediction," *Appl. Acoust.*, vol. 227, Jan. 2025, Art. no. 110183, doi: 10.1016/j.apacoust.2024.110183.

[15] A. Ongel, E. Kohler, and J. Harvey, "Principal components regression of onboard sound intensity levels," *J. Transp. Eng.*, vol. 134, no. 11, pp. 459–466, Nov. 2008, doi: 10.1061/(asce)0733-947x(2008)134:11(459).

[16] H. Bendtsen, Q. Lu, and E. Kohler, "Temperature influence on road traffic noise: Californian OBSI measurement study," Univ. California Pavement Res. Center (UCPRC), Davis, CA, USA, Rep. UCPRC-RP-2010-02, May 2010.

[17] T. D. Rossing, *Springer Handbook of Acoustics*. New York, NY, USA: Springer, 2014, doi: 10.1007/978-1-4939-0755-7.

[18] Y. Yoon, J. Lee, K. Yum, S. K. Lee, and S. Hwang, "Development of a prediction model for tire tread pattern noise based on convolutional neural network with RMSProp algorithm," in *Proc. WCX SAE World Congr. Exper., Detroit Online*, 2022, doi: 10.4271/2022-01-0884.

[19] R. Burdzik and D. Khan, "An overview of the current state of knowledge and technology on techniques and procedures for signal processing, analysis, and accurate inference for transportation noise and vibration," *Measurement*, vol. 252, Aug. 2025, Art. no. 117314, doi: 10.1016/j.measurement.2025.117314.

[20] S. E. Paje, M. Bueno, F. Terán, and U. Viñuela, "Monitoring road surfaces by close proximity noise of the tire/road interaction," *J. Acoust. Soc. Amer.*, vol. 122, no. 5, pp. 2636–2641, Nov. 2007, doi: 10.1121/1.2766777.

[21] L. Rapino, L. Liu, A. Dinosio, F. Ripamonti, R. Corradi, and S. Baro, "Processing of tyre data for rolling noise prediction through a statistical modelling approach," *Mech. Syst. Signal Process.*, vol. 188, Apr. 2023, Art. no. 110042, doi: 10.1016/j.ymssp.2022.110042.

[22] T. Li, "Literature review of tire-pavement interaction noise and reduction approaches," *J. Vibroengineering*, vol. 20, no. 6, pp. 2424–2452, Sep. 2018.

[23] Q. Li, F. Ripamonti, R. Corradi, and M. Caccialanza, "Simulation of deterministic tyre noise based on a monopole substitution model," *Appl. Acoust.*, vol. 178, Jul. 2021, Art. no. 108009, doi: 10.1016/j.apacoust.2021.108009.

[24] J. Pinay, H.-J. Unrau, and F. Gauterin, "Prediction of close-proximity tire-road noise from tire cavity noise measurements using a statistical approach," *Appl. Acoust.*, vol. 141, pp. 293–300, Dec. 2018, doi: 10.1016/j.apacoust.2018.07.023.

[25] S. Mohammadi and A. Ohadi, "Introducing a procedure for predicting and reducing tire/road noise using a fast-computing hybrid model," *J. Acoust. Soc. Amer.*, vol. 151, no. 3, pp. 1895–1912, Mar. 2022, doi: 10.1121/10.0009751.

[26] P. Gautam, Y. Azizi, and A. Chandy, "Developing a statistical model to predict tire noise at different speeds," *SAE Int. J. Vehicle Dyn., Stability, NVH*, vol. 1, no. 2, pp. 198–203, Mar. 2017, doi: 10.4271/2017-01-1507.

[27] M. Ohiduzzaman, O. Sirin, and E. Kassem, "Assessment of tire-pavement noise by using on-board sound intensity (OBSI) method in the State of Qatar," in *Bearing Capacity of Roads, Railways and Airfields*. Boca Raton, FL, USA: CRC Press, 2017, pp. 953–959.

[28] D. Chen, C. Ling, T. Wang, Q. Su, and A. Ye, "Prediction of tire-pavement noise of porous asphalt mixture based on mixture surface texture level and distributions," *Construction Building Mater.*, vol. 173, pp. 801–810, Jun. 2018, doi: 10.1016/j.conbuildmat.2018.04.062.

[29] T. Li, R. Burdisso, and C. Sandu, "An artificial neural network model to predict tread pattern-related tire noise," SAE Tech. Paper 2017-01-1904, Jun. 2017, vol. 1, doi: 10.4271/2017-01-1904.

[30] S.-K. Lee, H. Lee, J. Back, K. An, Y. Yoon, K. Yum, S. Kim, and S.-U. Hwang, "Prediction of tire pattern noise in early design stage based on convolutional neural network," *Appl. Acoust.*, vol. 172, Jan. 2021, Art. no. 107617, doi: 10.1016/j.apacoust.2020.107617.

[31] P. Dai, R. Dai, Y. Yin, J. Wang, H. Huang, and W. Ding, "A novel empirical-informed neural network method for vehicle tire noise prediction," *Machines*, vol. 13, no. 10, p. 911, Oct. 2025, doi: 10.3390/machines13100911.

[32] Y. Ma, R. Dai, T. Liu, M. Wang, Q. Ying, and H. Huang, "Physics-informed GRU model for vehicle road noise prediction: Integrating transfer path analysis and hybrid data," *Sound Vib.*, vol. 59, no. 3, p. 3143, Jul. 2025, doi: 10.59400/sv3143.

[33] C. Liang, M. Hao, Y. Shen, H. Li, and J. Fan, "Tire noise prediction based on transfer learning and multi-modal fusion," *Proc. Inst. Mech. Eng., D, J. Automobile Eng.*, vol. 239, no. 6, pp. 1959–1969, May 2025, doi: 10.1177/09544070241232606.

[34] Y. Che, W. X. Xiao, L. J. Chen, and Z. C. Huang, "GA-BP neural network based tire noise prediction," *Adv. Mater. Res.*, vols. 443–444, pp. 65–70, Jan. 2012, doi: 10.4028/www.scientific.net/amr.443-444.65.

[35] S. J. Hong, S.-W. Park, and S. W. Lee, "Tire-pavement noise prediction using asphalt pavement texture," *KSCE J. Civil Eng.*, vol. 22, no. 9, pp. 3358–3362, Sep. 2018, doi: 10.1007/s12205-018-9501-3.

[36] D.-H. Shen, C.-M. Wu, and J.-C. Du, "Application of grey model to predict acoustical properties and tire/road noise on asphalt pavement," in *Proc. IEEE Intell. Transp. Syst. Conf.*, Toronto, ON, Canada, 2006, pp. 175–180, doi: 10.1109/ITSC.2006.1706738.

[37] J.-T. Chiu and F.-Y. Tu, "Application of a pattern recognition technique to the prediction of tire noise," *J. Sound Vib.*, vol. 350, pp. 30–40, Aug. 2015, doi: 10.1016/j.jsv.2015.04.013.

[38] L. Spies, T. Li, R. Burdisso, and C. Sandu, "An artificial neural network (ANN) approach to model tire-pavement interaction noise (TPIN) based on tire noise separation," *Appl. Acoust.*, vol. 206, Apr. 2023, Art. no. 109294, doi: 10.1016/j.apacoust.2023.109294.

[39] I. K. Umar, M. Adamu, N. Mostafa, M. S. Riaz, S. I. Haruna, M. F. Hamza, O. S. Ahmed, and M. Azab, "The state-of-the-art in the application of artificial intelligence-based models for traffic noise prediction: A bibliographic overview," *Cogent Eng.*, vol. 11, no. 1, Dec. 2024, Art. no. 2297508, doi: 10.1080/23311916.2023.2297508.

[40] P. Cohrs and E. Chevalier, "Assessing, tyre-road noise, insights from texture analysis and acoustic characterization," in *Proc. DAGA*, 2025, pp. 794–797.

[41] G. Böttcher, C. Schliephake, V. Yordanov, and D. Werner, "Project tyre road noise-development of an estimation method for the pass-by noise," in *Proc. DAGA*, 2025, pp. 1473–1475.

[42] M. Demetgul, J. Meng, S. Lazarova-Molnar, and A. Vinel, "Data requirements for tire-road monitoring: A roadmap for data collection, processing, and decision making," in *Proc. IEEE 102nd Veh. Technol. Conf. (VTC-Fall)*, Chengdu, China, Oct. 2025, pp. 1–7, doi: 10.1109/VTC2025-FALL65116.2025.11310369.
[43] E. Freitas, J. Tinoco, F. Soares, J. Costa, P. Cortez, and P. Pereira, "Modelling tyre-road noise with data mining techniques," *Arch. Acoust.*, vol. 40, no. 4, pp. 547–560, Dec. 2015, doi: 10.1515/aoa-2015-0054.
[44] L. G. Del Pizzo, F. Bianco, A. Moro, G. Schiaffino, and G. Licitra, "Relationship between tyre cavity noise and road surface characteristics on low-noise pavements," *Transp. Res. D, Transp. Environ.*, vol. 98, Sep. 2021, Art. no. 102971, doi: 10.1016/j.trd.2021.102971.
[45] J. Masino, J. Pinay, M. Reischl, and F. Gauterin, "Road surface prediction from acoustical measurements in the tire cavity using support vector machine," *Appl. Acoust.*, vol. 125, pp. 41–48, Oct. 2017, doi: 10.1016/j.apacoust.2017.03.018.
[46] G. Schiaffino, L. G. Del Pizzo, S. Silvestri, F. Bianco, G. Licitra, and F. G. Praticò, "Machine learning techniques applied to road health status recognition through tyre cavity noise analysis," *J. Phys., Conf. Ser.*, vol. 2162, May 2022, Art. no. 012011, doi: 10.1088/1742-6596/2162/1/012011.
[47] A. E. Hoerl and R. W. Kennard, "Ridge regression: Biased estimation for nonorthogonal problems," *Technometrics*, vol. 12, no. 1, pp. 55–67, Feb. 1970, doi: 10.1080/00401706.1970.10488634.
[48] P. Geurts, D. Ernst, and L. Wehenkel, "Extremely randomized trees," *Mach. Learn.*, vol. 63, no. 1, pp. 3–42, Apr. 2006, doi: 10.1007/s10994-006-6226-1.
[49] L. Breiman, "Random forests," *Mach. Learn.*, vol. 45, no. 1, pp. 5–32, Oct. 2001, doi: 10.1023/a:1010933404324.
[50] D. E. Rumelhart, G. E. Hinton, and R. J. Williams, "Learning representations by back-propagating errors," *Nature*, vol. 323, no. 6088, pp. 533–536, Oct. 1986, doi: 10.1038/323533a0.

M. DEMETGÜL is currently a Postdoctoral Researcher with the Institute of Applied Informatics and Formal Description Methods (AIFB), Karlsruhe Institute of Technology (KIT). He is also a member of SYDSEN Research Group and works on the TireRoadNoise Project. Before joining AIFB, he was a Solution Developer for computer vision at ZEISS Innovation Hub KIT. Here, he carried out projects on computer vision and GANs. With the support of a scholarship from the Alexander Humboldt Foundation, he also did postdoctoral research with KIT WBK Institute, focusing on sensorless monitoring in machines and anomaly detection using computer vision and time series data. Before Germany, he gained experience in Türkiye and USA. From 2007 to 2009, he was a Postdoctoral Fellow with the Department of Mechanical Engineering, Florida International University (FIU), USA, where he worked on structural health monitoring and energy harvesting. Then, he was an Assistant Professor and later an Associate Professor with the Department of Mechatronics Engineering, Marmara University, Türkiye. During his tenure, he established and managed a laboratory dedicated to fault diagnosis and structural health monitoring. His research interests include artificial intelligence, anomaly detection, computer vision, predictive maintenance, signal processing, and structural health monitoring. He is on the editorial boards of several international journals and he has published extensively in international journals on anomaly and fault detection.

M. HEINZELMANN received the bachelor's degree in mathematics. He is currently pursuing the master's degree in mathematics with Karlsruhe Institute of Technology (KIT), Germany, with a focus on statistics, probability, and machine learning. He is also a Student Research Assistant with the Institute of Applied Informatics and Formal Description Methods, KIT. Within the SDYSEN Research Group, he is involved in the TireRoad-Noise Project, where he works on the development of data-driven approaches for analyzing and modeling tire–road interaction noise. He has contributed to recent research publications in this field. His academic interests include statistical modeling, uncertainty quantification, and the application of machine learning methods to real-world engineering problems.

S. LAZAROVA-MOLNAR is currently a Professor with the Institute of Applied Informatics and Formal Description Methods, Karlsruhe Institute of Technology, Germany. She is also a Professor with the Faculty of Engineering, University of Southern Denmark, Denmark. Her research interests include data-driven simulation, digital twins, and cyber-physical systems modeling for reliability and energy efficiency enhancement. Actively engaged in developing advanced methodologies, she leverages her expertise to optimize complex systems through data-driven simulation. She leads activities focused on digital twins and data-driven simulation in several European and national projects. She assumes leadership roles in IEEE and the Society for Modeling and Simulation International (SCS). She is also serving as a Representative of SCS to the Winter Simulation Conference (WSC) Board of Directors. She was also one of the Proceedings Editors for the Winter Simulation Conference, in 2019 and 2020. She is an Associate Editor of *SIMULATION: Transactions of the Society for Modeling and Simulation International*.